Proc. of the 2019 IEEE 6th International Conference on Smart Instrumentation, Measurement and Applications (ICSIMA 2019)
27-29 August 2019, Kuala Lumpur, Malaysia

Hybrid PSO-Tuned PID and Hysteresis-Observer Based Control for Piezoelectric Micropositioning Stages

Marwan Nafea[#1], Zaharuddin Mohamed[*2], Mohamed Sultan Mohamed Ali[*3], Kamyar Mehranzamir[#4], Tariq Rehman[*5]

[#]*Department of Electrical and Electronic Engineering, Faculty of Science and Engineering, University of Nottingham Malaysia*
43500 Semenyih, Selangor, Malaysia

[*]*School of Electrical Engineering, Faculty of Engineering, Universiti Teknologi Malaysia*
81310 Skudai, Johor, Malaysia

[1]marwan.nafea@nottingham.edu.my (Corresponding author), [2]zahar@fke.utm.my, [3]sultan_ali@fke.utm.my,
[4]kamyar.mehranzamir@nottingham.edu.my, [5]rtariq2@live.utm.my

***Abstract*—Piezo-actuated micropositioning stages consist of a piezoelectric actuator that operates a positioning system. Hysteresis nonlinearity is one of the significant variables limiting the positioning precision of these stages. This paper introduces a technique of developing a hybrid controller for a precise positioning tracking of a piezoelectric micropositioning system. Bouc-Wen nonlinear hysteresis model is utilized to denote the hysteresis nonlinear phenomenon of the piezo-actuated system. A hysteresis observer-based feedforward controller is designed based on Luenberger observer. This feedforward controller is then coupled with a particle swarm optimization (PSO)-based proportional-integral-derivative (PID) feedback controller to form a hybrid controller. A new fitness function is used to compute the optimal PID gains. This fitness function is intended to reduce the overshoot, steady-state error, and the rise and settling times. The findings of this work indicate that using the developed controller structure can significantly decrease the hysteresis effect. In addition, the proposed structure shows the ability to reduce the error is to 0.046% of the maximum displacement range. Such performance demonstrates that the proposed hybrid control structure is efficient for precise micropositioning applications.**

Keywords—PSO; PID; piezoelectric; Bouc-Wen; feedback; feedforward

I. INTRODUCTION

Micropositioning stages have been extensively implemented in various applications apps, including imaging tunneling microscopy, atomic force microscopy, optical bridge connections, and parallel test-based data storage systems. Various micropositioning stages with different actuation mechanisms and structures have been developed. Such actuating mechanisms include electrostatic [1], shape-memory-alloy [2], electromagnetic [3], electrothermal [4], and piezoelectric actuators [5]. The choice of the suitable type of microactuators depends on the specifications of the actuator and the system, the ability of the integration with the fabrication process, and the economic feasibility. One of the most important factors that should be taken in account to satisfy these conditions is the efficiency of the microactuator, which is the ratio of the mechanical work output to the energy input of the actuator during a complete operation cycle. Electrostatic microactuators are high efficient actuators, but their stroke is small, require very high voltage over narrow gaps between electrodes, and have a short lifetime, which limit the applications of the device [6]. Electromagnetic microactuators possess high efficiency, but they have limitations in terms of operation and material compatibility, as well as the integration of the magnetic materials into the overall fabrication process. Thermal and shape-memory-alloy microactuators have low efficiency and slower cycle rates than other types of microactuators [7]. Piezoelectric microactuators have the highest efficiency among other types of actuators. Furthermore, they have the advantages of and high stiffness, fast response, and high resolution in the nanometer range, which make them favorable to be used in micropositioning stages.

The primary shortcomings of piezoelectric actuators are nonlinearity induced by the creep phenomenon, high-frequency vibrations, and hysteresis [8]. Creep is a slight shift in the position after the required displacement when a steady voltage is applied to the terminals of the piezoelectric actuator. This behavior leads to a poor precision when positioning is required for a long time. Creep can be reduced by operating the piezoelectric actuator over a short duration of time. This phenomenon is often represented by a nonlinear logarithmic model of time and input voltage [9], or a linear dynamic model. On the other side, when a piezoelectric actuator is operated at frequencies near to its first resonant frequency, unwanted vibrations occur. This limits the operating frequencies of the piezoelectric actuator to less than 1% to 10% of the first resonant frequency [10]. These vibrations are usually simulated and compensated depending on the identified dynamics of the piezoelectric actuator [11]. While hysteresis produces severe nonlinear effects on the movement of piezoelectric actuator, the nonlinear effects of creep and near-resonant vibrations are comparatively low. The nonlinear relationship that relates the applied voltage and the produced displacement creates problems in regulating the displacement of the piezoelectric actuator [12]. Charge-driven method was utilized by several

This work was supported by the University of Nottingham Malaysia, Prototype Research Grant Scheme (PRGS) 4L690 by the Ministry of Education Malaysia, and UTM Shine 04G75 by Universiti Teknologi Malaysia.

researchers to overcome the hysteresis issue. The use of charge-driven piezoelectric actuators was first proposed by Comstock in 1981, where a non-inverting charge feedback amplifier was used to supply a piezoelectric actuator with charge proportional to the voltage input of the amplifier. The main disadvantage of this method that it requires more voltage compared to the voltage driven method. In addition, , the use of these amplifiers increases the complexity of the charge control circuit and makes the implementation of this method more difficult and expensive compared to voltage driven method.

Before developing a system for hysteresis compensation, precise modeling of hysteresis should be carried out to tackle these problems. date, several hysteresis models have been proposed. These models can be categorized into physical and mathematical models. Physical models are derived based on the mechanism of hysteresis of the piezoelectric actuator, and they are often complicated; whereas mathematical models can be classified into static and dynamic models. Preisach, Prandtl-Ishlinskii, and the polynomial models are considered as static hysteresis models, while Duhem, Bouc-Wen, and Maxwell slip models are considered as dynamic hysteresis models [13]. Dynamic hysteresis designs are considered to be more accurate in representing the nonlinear hysteresis behavior of piezoelectric actuators. Bouc-Wen hysteresis model is a relatively simple model with fewer parameters that provide an outstanding capacity to precisely model any nonlinearity and a high ability to model non-symmetrical hysteresis loops. Despite the existence of such models, the tracking performance of piezoelectric actuators still suffers from the effects of hysteresis.

Several researchers have proposed various control techniques, such as hysteresis inversion, and two-degree-of-freedom control methods to overcome the hysteresis nonlinearity. However, there are still limitations in controlling micropositioning stages for precision positioning applications, due to the high nonlinearity of such systems. Motivated by the aforementioned challenges, this paper presents a two-degree-of-freedom control technique that utilizes a hysteresis observer-based feedforward controller and a proportional-integral-derivative (PID) feedback controller that is tuned using particle swarm optimization (PSO). The results show that the proposed technique offers a high-tracking performance and has the ability to achieve a linear relationship between the input and the output of the micropositioning system.

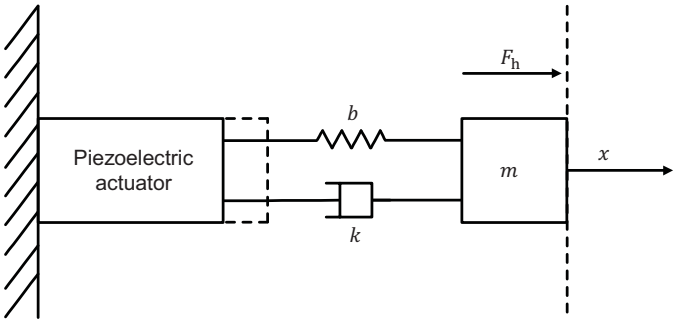

Fig. 1. Block diagram of the micropositioning system.

II. Modeling and Control of the System

The micropositioning system studied in this work is presented in Fig. 1. The system consists of a moving stage that is operated by a piezoelectric stack actuator. One tip of the piezoelectric actuator is attached and the other tip slides horizontally to push and pull the stage. Bouc-Wen hysteresis model is employed to depict the hysteresis behavior of the piezoelectric actuator. The hysteresis model of the piezo-actuated stage can be described using the following equation:

$$m\ddot{x} + b\dot{x} + kx = F_h = k(du - h) + F_{ext} \quad (1)$$

$$\dot{h} = \alpha d\dot{u} - \beta|\dot{u}|h - \gamma\dot{u}|h| \quad (2)$$

where x is the displacement of the piezo-actuated system, h is the hysteresis nonlinear component. The time derivatives of x are $\dot{x}, \ddot{x}$, while the derivative of h is given as $\dot{h}$. The mass, damper coefficient, and stiffness factor of the system are represented by m, b, and k, respectively. The applied voltage is represented by u, and the force generated by the piezoelectric actuator is denoted by F_h. In addition, the piezoelectric material constant is represented by d, and F_{ext} is the external force exerted by the load. The shape and the amplitude of the hysteresis loop are controlled by the parameters α, β and γ, where $0 < \alpha < 1$. The aforementioned equations of the micropositioning system can be represented in a state-space form, as previously presented in [9].

In this work, a hysteresis-observer based feedforward controller is utilized alongside a feedback PID controller to eliminate the hysteresis of the system. The design of the feedforward controller for the piezo-actuated system needs an observer to monitor the hysteresis. In fact, the issue of speed estimation can likewise be handled by utilizing the hysteresis state observer to assess the speed of the micropositioning system. This will give the chance to exclude speed sensors, reduce the cost, and eliminate sensor noise. The hysteresis of

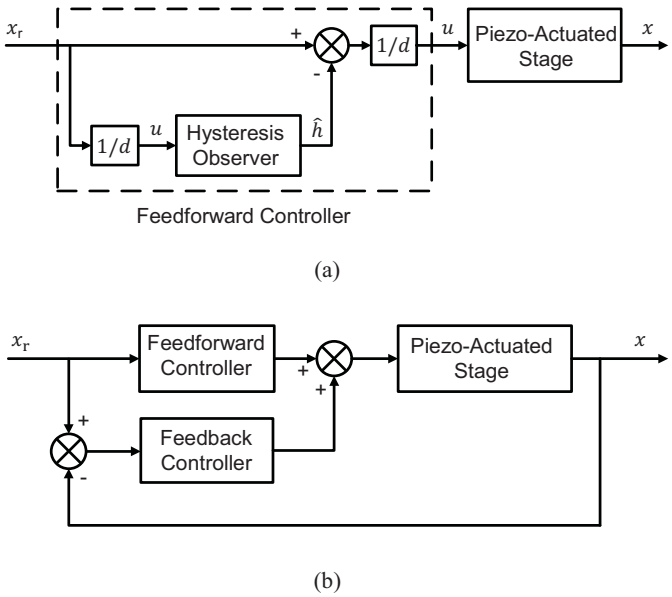

Fig. 2. Block diagram of (a) the feedforward controller. (b) Hybrid controller.

the piezo-actuated system is monitored with a Luenberger observer since this observer is easy to be designed and offers an efficient performance. A block diagram for the piezo-actuated system with an observatory-based feedforward controller is presented in Fig. 2(a). The Luenberger observer output is then coupled with the initial reference input (x_r) to form a feedforward controller that compensates for the nonlinearity of hysteresis.

The hybrid control structure is used to enhance the tracking efficiency and to minimize errors induced by hysteresis due to the large nonlinearity of this system. This technique is adequate for controlling piezo-actuated systems for high-accuracy positioning applications. The hybrid control is created by merging the feedforward controller with a PID feedback controller, as presented in Fig. 2(b). The PID gains (K_P, K_I, and K_D) are tuned to minimize the overshoot, steady-state error, and rise and settling times in order to design the PID controller for such a system. In this study, the optimal PID gains are computed using PSO to overcome the challenges of tuning the gains of the controller of such highly nonlinear system. Each location in the d-dimensional search space represents a possible location of the solution of the gains tuning process. In addition, every particle is regarded as a point in the search space, where x and v are the velocity and position the of that particle, respectively. The best previous position (according to the fitness function presented later) is given as $pbest_i$ and the index of the best particle of all particles in the population is expressed as $gbest_d$. Then, the solution can be found using the following equations:

$$v_{i,d}(t+1) = w.v_{i,d}(t) + c_1 * r_1 * (pbest_{i,d}(t) - x_{i,d}(t)) + c_2 * r_2 * (gbest_d(t) - x_{i,d}(t)) \quad (3)$$

$$x_{i,d}(t+1) = x_{i,d}(t) + v_{i,d}(t+1), i = 1,2,\ldots,n,\ d = 1,2,\ldots,q \quad (4)$$

where t is the index of generations, n is the number of particles in a group, and q is the number of members in a particle. The velocity of a particle i at iteration t is given as $v_{i,d}(t)$, where $v_d^{\min} \le v_{i,d} \le v_d^{\max}$. The intertie weight factor is denoted by w, and c_1 and c_2 are the acceleration factors, while r_1 and r_2 are random numbers between 0 and 1. The position of a particle i at iteration t, is given as $x_{i,d}(t)$, where $x_d^{\min} \le x_{i,d} \le x_d^{\max}$.

In the above definitions, the minimum and maximum velocity values are restricted between two constraints, $v_d^{\min}$ and $v_d^{\max}$, respectively. The $v_d^{\max}$ parameter indicates the search resolution between the present location and the destination location in the search area. Too high values of $v_d^{\max}$ might lead the particles to pass good solution. On the other hand, too small values might limit exploring new good solutions beyond locally good regions, or even stuck in local optima [9]. Thus, the value of $v_d^{\max}$ is often specified to be 50% of the possible solution range of the variable. The parameters $x_d^{\min}$ and $x_d^{\max}$ are the minimum and peak limits of the particle place on each dimension. These parameters are set to be in the feasible solution spectrum. The constants c_1 and c_2 are respectively the variable of cognitive acceleration and the variable of social acceleration. These constants scale the impact of p_{best} and g_{best} on the result. Low values enable particles to discover new areas far from the goal before being drawn back, while high scores cause particles to migrate unexpectedly to new search areas. Thus, these constants are often fixed to be 2.0 to match local and global exploration, as their median holds the weights for cognitive and social components equivalent to 1.0. In addition, in order to control the trade-off between the local and global explorations for various search problems, the inertia weight w is generally reduced gradually from 0.9 to 0.4 during the search according to the subsequent formula:

$$w = \frac{w_{\max} - w_{\min}}{iter_{\max}} \times iter \quad (5)$$

In the previous equation, the lowest and highest values of the inertia weight are represented by $w_{\min}$ and $w_{\max}$, respectively. In addition, the maximum number of iterations and the number of the current iteration are given as $iter_{\max}$ and $iter$, respectively.

III. Results and Discussion

In this work, the values of the parameters of the piezo-actuated micropositioning stage are adopted from a previous work [14], as presented in Table I. A 1 Hz triangular voltage signal with an amplitude of 80 V is used to operate the piezoelectric actuator. A feedforward controller is then utilized to enhance the output tracking performance of the piezo-actuated stage. The hybrid control structure is implemented in order to achieve a precise positioning while operating the piezo-actuated stage. This controller has the ability to improve the tracking performance of the micropositioning system and reduce errors caused by the nonlinearities and inaccurate modeling. The hybrid control structure is composed of the hysteresis observer-based feedforward controller and the PSO-based PID feedback controller. In this paper, a new fitness function in the time domain is suggested to evaluate the performance of the PID controller. An efficient PID controller yields a good step response with minimal performance criteria in the time domain. These performance criteria include the rise time (t_r), settling time (t_s), steady-state error (E_{SS}), and overshoot (M_P). Thus, the fitness function, f is presented using the following equation:

$$f = 10^{\delta} \frac{M_P + E_{ss}}{t_s - t_r} \quad (6)$$

where δ is the weighting factor. The fitness function can be adjusted to meet the designer requirements using the value of δ. Increasing the value of δ has a positive effect on the overshoot and steady-state error, while decreasing it has a positive effect

TABLE I. Values of the piezo-actuated system parameters.

Parameter	Value	Parameter	Value
b	4378.67 Ns/m	F_{ext}	0 N
k	3×10^5 N/m	α	0.38
d	9.013×10^{-7} m/V	β	0.0335
m	2.17 kg	γ	0.0295

on the rise time and settling time. Selecting the suitable value of δ is decided according to previous knowledge of the dynamic performance of the system. The proposed fitness function provides a tunable trade-off between the performance criteria in the time domain.

The performance of the hybrid controller is implemented by MATLAB/Simulink, and executed on an Intel Core i7 2.5 GHz with 16 GB RAM computer. A step input with an amplitude of 80 V is used to test the time-domain performance criteria (t_r, t_s, E_{SS}, and M_P), while 3 simulation examples are carried out to evaluate the performance of the hybrid controller based on those criteria, where each example has a different population size. In the first example, δ is set to be 100 to balance between the overshoot and steady-state error on one side, and the rise time and settling time on the other, as described earlier in (6). Then, the value of δ is increased to observe its effect on the tuning process. The population size and number of iterations are set to be 20 in the simulation examples. The values of the population size are selected based on previous experience, where these values fall in the range that convergence occurs. In addition, increasing the population size will increase the computation cost of the simulation process. Additionally, 20 trials of each simulation example are performed with different random numbers to study the variation of their evaluation values. The simulation results of these examples are summarized in Table II. As indicated by Table II, the second simulation example with a weighting factor δ of 200 gives the fastest time response and the lowest overshoot and steady-state error, which makes it the best solution. The performance of the controller can be tuned by varying the value of δ, which demonstrates the flexibility of the proposed fitness function and its ability to handle highly-nonlinear control problems.

Further observations of the values of the PID gains in each generation (iteration) of the second example show that those gains do not require many iterations to converge to their best solution, where the gains converged after the fifth iteration, as shown in Fig. 3. Thus, the minimum possible evaluation value could be achieved as fast as those gains reach to their best solution. Such observations demonstrate the ability of the proposed fitness function to tune highly nonlinear system that are controlled using PID. Furthermore, the proposed fitness function is utilized to track the aforementioned triangular input voltage to test the performance of the micropositioning system, where the sharp edges of the triangular signal push the micropositioning system to its limit and test the ability of the proposed controller. The hybrid trajectory tracking control response is illustrated in Fig. 4. It can be indicated from the figure that the output displacement of the open-loop system shows a phase lagging and tracking errors on the rising and falling slopes of the signal, which is caused by the nonlinear relationship between the applied voltage and the generated displacement of the piezoelectric actuator [15]. On the other hand, the output of the controlled system shows that the displacement is almost identical to the input signal, with a significantly low error value. Moreover, the tracking error signal of the open-loop and hybrid-controlled systems are illustrated in Fig. 5. By comparing the two errors peaks values, it can be indicated that the error has decreased from -743 nm to 750 nm, for the open-loop system, to -33.4 nm and 33 nm, when the hybrid controller was used. These results illustrate that the tracking error has decreased from 10.41% to 0.046% of the maximum displacement, which show an enhancement in the tracking performance by 99.56% when compared to the open-loop system. It should be noted that the error can be

TABLE II. Comparison of the performance of the tuned controllers at different δ values.

δ	K_P	K_I	K_D	t_r (ms)	t_s (ms)	M_P (%)	E_{SS} (µm)
100	141.520	38.318	0.052	0.764	0.993	0.012	0.019
200	149.745	46.411	0.054	0.740	0.964	0.011	0.017
300	146.965	48.736	0.055	0.743	0.968	0.014	0.018

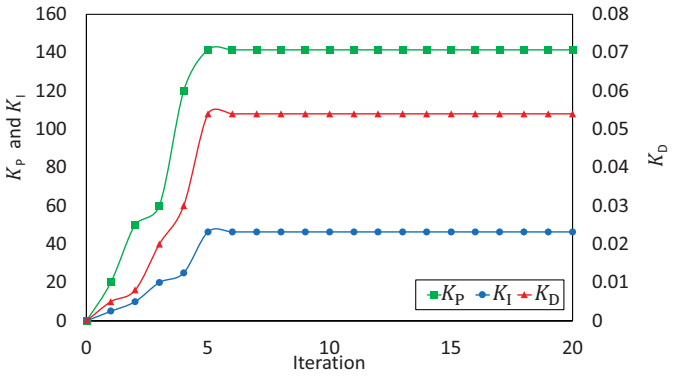

Fig. 3. PID gains convergence results.

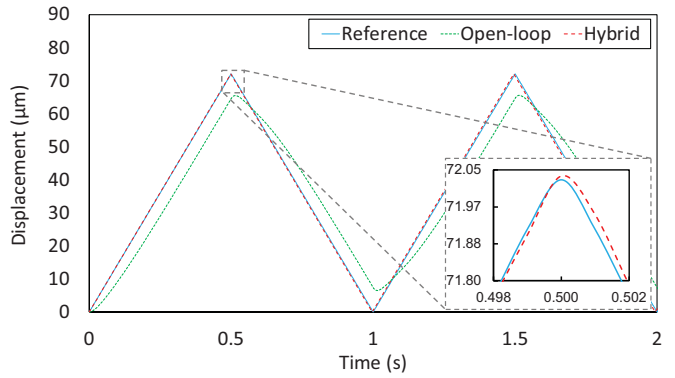

Fig. 4. Output responses of the open-loop and controlled systems compared with the reference signal.

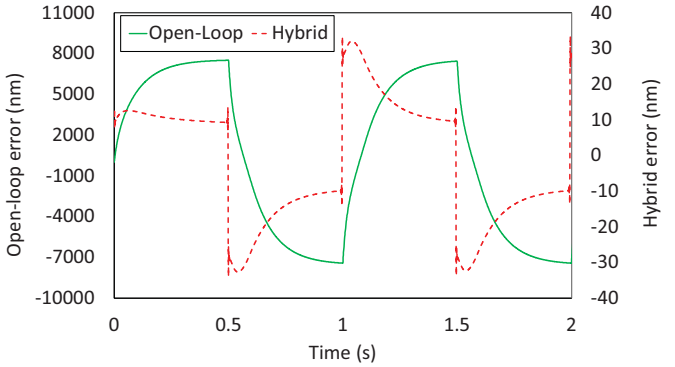

Fig. 5. Tracking errors of the open-loop and controlled systems.

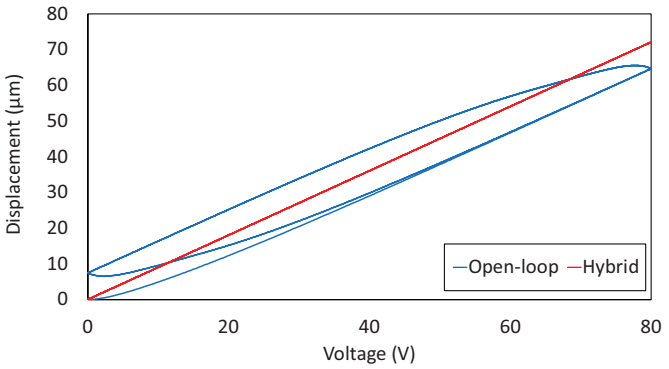

Fig. 6. Hysteresis relationships of the open-loop and controlled systems.

further reduced by increasing the upper limit of the search space of the PSO algorithm. However, such action must be governed by the voltage limitations of the piezoelectric actuator, where in several cases, a saturation limit is used at the terminals of the piezoelectric actuator to prevent excessive voltage values from damaging it.

For further investigation of the performance of the proposed controller, the relationship between the input and output of the system is illustrated in Fig. 6, which shows the hysteresis nonlinear relationship between the voltage and the displacement of the open-loop and hybrid-controlled micropositioning system. It can be seen that as the tracking error is reduced when the hybrid controller is implemented, the relationship between the voltage and the displacement is linearized. In addition, it can be seen that the displacement range of the controlled system has increased, since the proposed controller allowed the output of the system to track the input signal. These observations agree well with the results presented in Fig. 4.

These observations demonstrate the efficiency of the proposed concept, making this system suitable to be used in various high-precision positioning applications. It can be concluded that the feedforward controller plays an important role in reducing the hysteresis according the observed hysteresis state, while the feedback controller eliminates the modeling errors, coupling effect and other uncertainties. These two controllers combined achieved the desired task of eliminating the hysteresis level up to a significant leven. It is worth mentioning that a similar hybrid control approach can be used to control such system by implementing resonant control methods [16] or by replacing the hysteresis observer-based feedforward controller with a hysteresis inversion-based feedforward controller [17] and implementing a similar PSO-based tuning approach.

IV. Conclusion

This paper presented a method for designing a hybrid controller for precise positioning of a piezoelectric actuator micropositioning stages. The model of the piezo-actuated stage was presented using the Bouc-Wen hysteresis model. A hysteresis observer-based feedforward controller was designed based on Luenberger observe structure. This feedforward controller was then combined with a PSO-based PID feedback controller to form a hybrid controller. The system was simulated using MATLAB/Simulink and the optimal PID gains were then obtained using a new fitness function that is proposed to enhance the tracking performance of the micropositioning system. The results showed that the hysteresis effect was significantly decreased using the proposed control structure, where the maximum error was minimized to ~33 nm, which is about 0.046% of the maximum displacement, while achieving rise and settling times of 0.740 ms and 0.964 ms, respectively. Future work will involve performing system identification of several piezo-actuated systems and comparing the modeling results of Bouc-Wen model with other models, such as Preisach model. The proposed optimization method can be further implemented in various micropositioning and sensitive biomedical applications, such as finding the optimal design and optimal control of drug delivery devices [18]. Further improvement of the tracking performance of the system can be achieved in the future by using adaptive control strategies that utilize hysteresis inversion, as well as using different optimization methods, such as gravitational search algorithm.

References

[1] M. Olfatnia, L. Cui, P. Chopra, and S. Awtar, "Large range dual-axis micro-stage driven by electrostatic comb-drive actuators," *J. Micromech. Microeng.,* vol. 23, p. 105008, 2013.

[2] A. AbuZaiter, O. F. Hikmat, M. Nafea, and M. S. M. Ali, "Design and fabrication of a novel XYθz monolithic micro-positioning stage driven by NiTi shape-memory-alloy actuators," *Smart Mater. Struct.,* vol. 25, 2016.

[3] S. Xiao, Y. Li, and J. Liu, "A model reference adaptive PID control for electromagnetic actuated micro-positioning stage," in *2012 IEEE Int. Conf. Autom. Sci. Eng. (CASE)*, 2012, pp. 97-102.

[4] M. Rakotondrabe, A. G. Fowler, and S. R. Moheimani, "Control of a novel 2-dof MEMS nanopositioner with electrothermal actuation and sensing," *IEEE Trans. Control Syst. Technol.,* vol. 22, pp. 1486-1497, 2013.

[5] M. Nafea, C. Schlosser, S. Kazi, Z. Mohamed, and M. S. Mohamed Ali, "Optimal two-degree-of-freedom control for precise positioning of a piezo-actuated stage," *Int. J. Integr. Eng.,* vol. 9, pp. 93-102, 2017.

[6] R. Pelrine, R. Kornbluh, J. Joseph, R. Heydt, Q. Pei, and S. Chiba, "High-field deformation of elastomeric dielectrics for actuators," *Mater. Sci. Eng., C,* vol. 11, pp. 89-100, 2000.

[7] M. Nafea, A. AbuZaiter, S. Kazi, and M. S. M. Ali, "Frequency-controlled wireless passive thermopneumatic micromixer," *J. Microelectromech. Syst.,* vol. 26, pp. 691-703, 2017.

[8] T. J. Yeh, H. Ruo-Feng, and L. Shin-Wen, "An integrated physical model that characterizes creep and hysteresis in piezoelectric actuators," *Simul. Modell. Pract. Theory,* vol. 16, pp. 93-110, 2008.

[9] M. Nafea, S. Kazi, Z. Mohamed, and M. S. Mohamed Ali, "A hybrid control approach for precise positioning of a piezo-actuated stage," in *2014 14th Int. Conf. Control, Autom. Syst. (ICCAS)*, Seoul, South Korea, 2014, pp. 667-671.

[10] D. Croft, G. Shed, and S. Devasia, "Creep, hysteresis, and vibration compensation for piezoactuators: Atomic force microscopy application," *J. Dyn. Syst. Meas. Contr.,* vol. 123, pp. 35-43, 2001.

[11] H. Habibullah, H. Pota, I. R. Petersen, and M. Rana, "Creep, hysteresis, and cross-coupling reduction in the high-precision positioning of the piezoelectric scanner stage of an atomic force microscope," *IEEE Trans. Nanotechnol.,* vol. 12, pp. 1125-1134, 2013.

[12] M. Nafea, A. Nawabjan, and M. S. Mohamed Ali, "A wirelessly-controlled piezoelectric microvalve for regulated drug delivery," *Sens. Actuators, A,* vol. 279, pp. 191-203, 2018.

[13] G. Y. Gu, L. M. Zhu, C. Y. Su, H. Ding, and S. Fatikow, "Modeling and control of piezo-actuated nanopositioning stages: A survey," *IEEE Trans. Autom. Sci. Eng.,* vol. 13, pp. 313-332, 2016.

[14] M. Nafea, Z. Mohamed, A. M. Abdullahi, M. R. Ahmad, and A. R. Husain, "Dynamic hysteresis based modeling of piezoelectric actuators," *J. Teknol.,* vol. 67, pp. 9-13, 2014.
[15] J. Peng and X. Chen, "Novel models for one-sided hysteresis of piezoelectric actuators," *Mechatronics,* vol. 22, pp. 757-765, 2012.
[16] A. M. Abdullahi, Z. Mohamed, and M. Nafea, "Resonant control of a single-link flexible manipulator," *J. Teknol.,* vol. 67, pp. 35-39, 2014.
[17] S. Xiao and Y. Li, "Dynamic compensation and h∞ control for piezoelectric actuators based on the inverse bouc–wen model," *Robot. Com. Int. Manuf.,* vol. 30, pp. 47-54, 2014.
[18] M. Nafea, A. AbuZiater, O. Faris, S. Kazi, and M. S. Mohamed Ali, "Selective wireless control of a passive thermopneumatic micromixer," in *2016 IEEE 29th Int. Conf. Micro Electro Mech. Syst. (MEMS)*, Shanghai, China, 2016, pp. 792-795.